Constraining the detectability of water ice in debris disks

M. Kim[1], S. Wolf[1], A. Potapov[2], H. Mutschke[3] & C. Jäger[2]

[1] **P4**: ITAP, Christian-Albrechts-Universität zu Kiel
[2] **P8**: MPIA, IFK, Friedrich-Schiller-Universität Jena
[3] **P6**: AIU, Friedrich-Schiller-Universität Jena

Ice detection in debris disks

- Observation of water ice features in 3 μm

Ice detection in debris disks

- Observation of water ice features in 3 $\mu\mathrm{m}$
- Other constraints from 44 and 62 $\mu\mathrm{m}$ observations

Ice detection in debris disks

- Observation of water ice features in 3 $\mu\mathrm{m}$
- Other constraints from 44 and 62 $\mu\mathrm{m}$ observations
- Abundant water ice detection in molecular clouds, protoplanetary disks, and likely **in outer planetary systems**

Future instrumentation

- Observation of water ice features in 3 $\mu\mathrm{m}$
  $\rightarrow$ JWST NIRCam (aiming for 0.6 to 5 $\mu\mathrm{m}$)

- Other constraints from 44 and 62 $\mu\mathrm{m}$ observations
  $\rightarrow$ SPICA SAFARI (aiming for 34 to 230 $\mu\mathrm{m}$)

- **Significant progress on our understanding about the ice in the debris disks by next-generation observatories**

Main question

Which are the observational requirements either ...

- to constrain the detectability of ice in debris disks or
- to provide useful limits for the existence, properties, and spatial distribution of ice in debris disks ?

Numerical methods: Model parameters

Parameters	Values
Stellar type	β - Pic like A6 V with 1.75 $M_\odot$, R = 1.8 $R_\odot$, and 8052 K (Mamajek 2002)
R_{in} and R_{out}	3 au and 150 au
Distance to the debris disks system	19.3 pc
Size range modeling $n(a)$	[0.1 μm, 1000 μm] with $n(a) \propto a^{-3.5}$ (Dohnanyi 1969)
Chemical component	Amorphous water ice (Li & Greenberg 1998; **Potapov+ 2018b**; Curtis+ 2005)
	Crystalline water ice (Curtis+ 2005; **Reinert+ 2015**; **Häßner+ 2018**; **Potapov+ 2018b**)
	Astrosilicate (Draine 2003)
Various dust aggregates	Spherical shape of astrosilicate matrix-ice inclusion
MG rule of EMT calculation with the **emc** code	Spherical shape of astrosilicate core-ice mantle
(Ossenkopf 1991)	Spherical shape of porous ice
	Platelets shape of astrosilicate matrix-ice inclusion
Fractional ratio of ice $\mathcal{F}_{ice}$	0, 0.25, 0.5, 0.75, and 1
Different mechanism of ice destruction	Sublimation, UV photosputtering, and collision

Simulated observations : **DMS** (**D**ebris around **M**ain-sequence **S**tars; Kim et al. 2018)

1-1. SED: Impact of ice destruction mechanism

Strong influence of different ice destruction mechanisms, e.g., UV photosputtering, collisions, and sublimation, on the SED

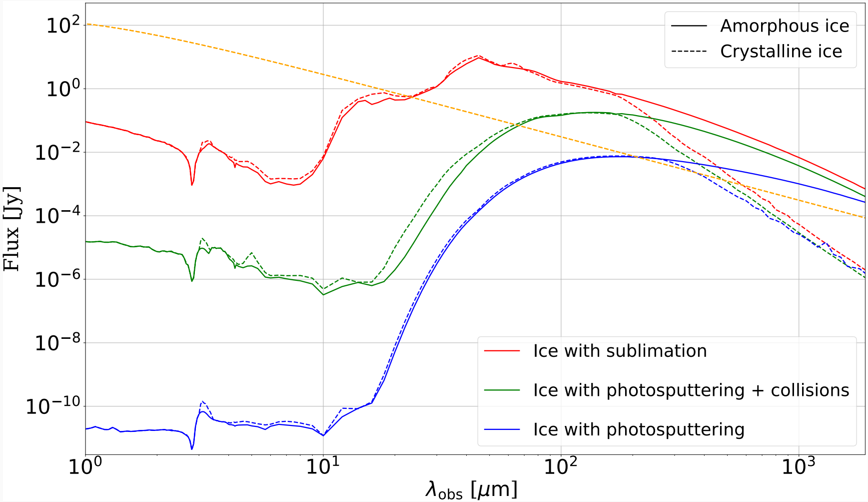

1-1. SED: Impact of ice destruction mechanism

Destruction of small size ice →significantly decreased scattered radiation at the near-IR to mid-IR

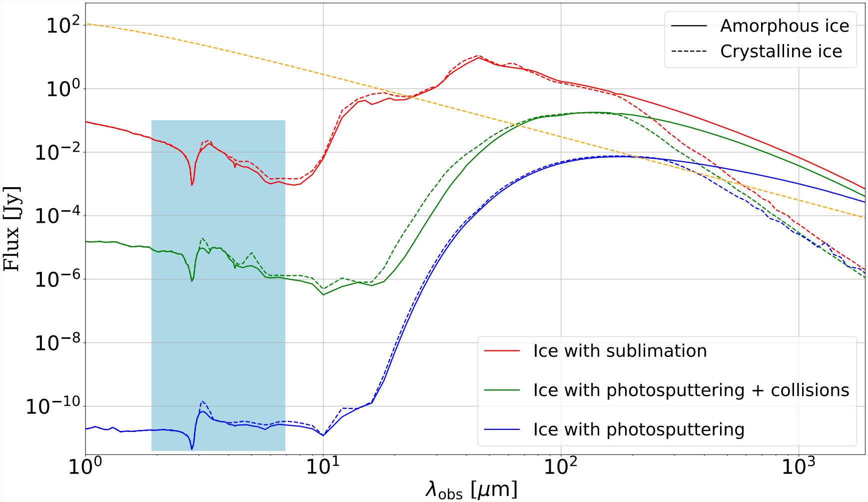

1-1. SED: Impact of ice destruction mechanism

Significant erosion of ice grain by UV photosputtering (and collision) far beyond the sublimation line

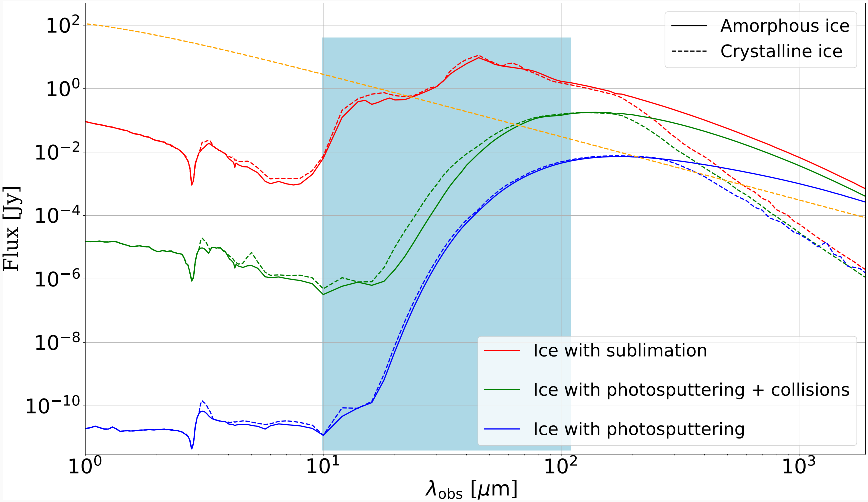

1-1. SED: Impact of ice destruction mechanism

Less efficient contribution of UV photosputtering (and collision) to the destruction of bigger grains

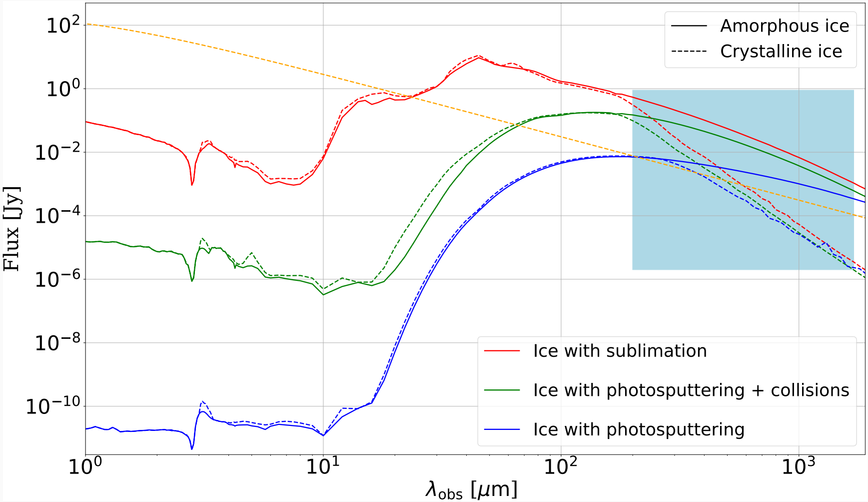

1-1. SED: Impact of $\mathcal{F}_{ice}$ in Astrosil + ice mixtures

$\mathcal{F}_{ice}$ is responsible for various features on the SED.

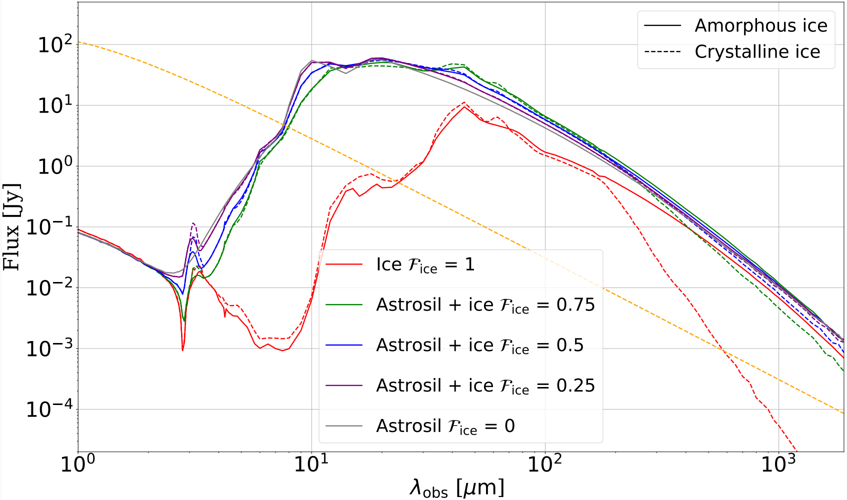

1-1. SED: Impact of $\mathcal{F}_{ice}$ in Astrosil + ice mixtures

Ice-poor $\longrightarrow$ shallow peak strength of 3 μm ice feature

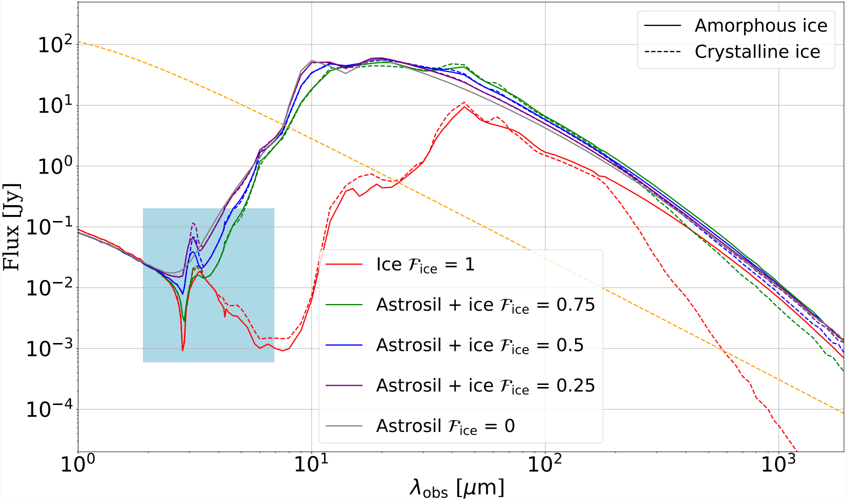

1-1. SED: Impact of $\mathcal{F}_{ice}$ in Astrosil + ice mixtures

Where is 10 μm silicate feature?

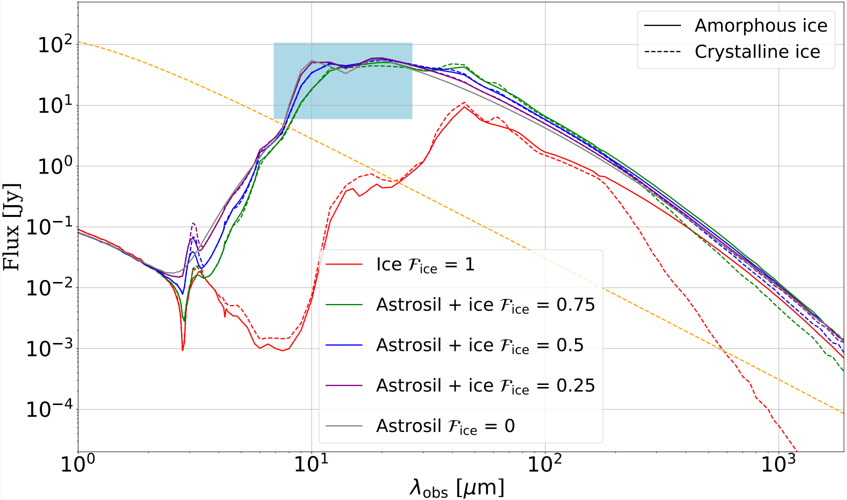

1-1. SED: Impact of $\mathcal{F}_{ice}$ in Astrosil + ice mixtures

44 and 62 μm ice features

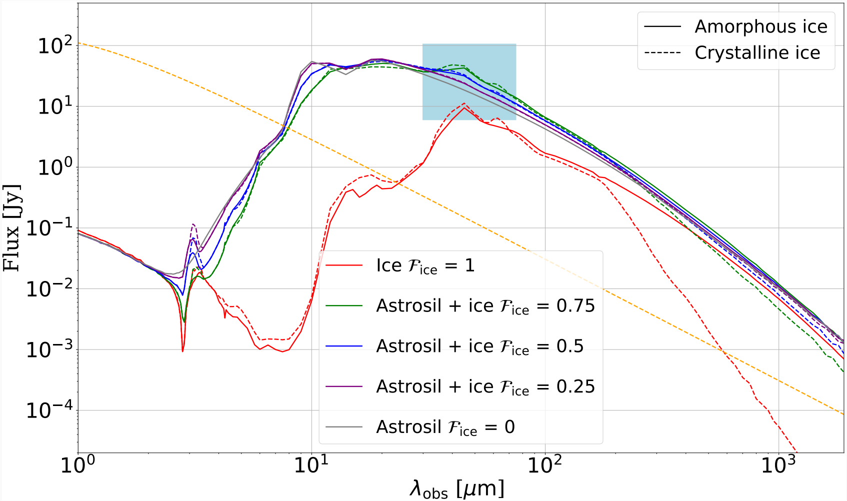

Highly polarized radiation of 3 μm ice feature

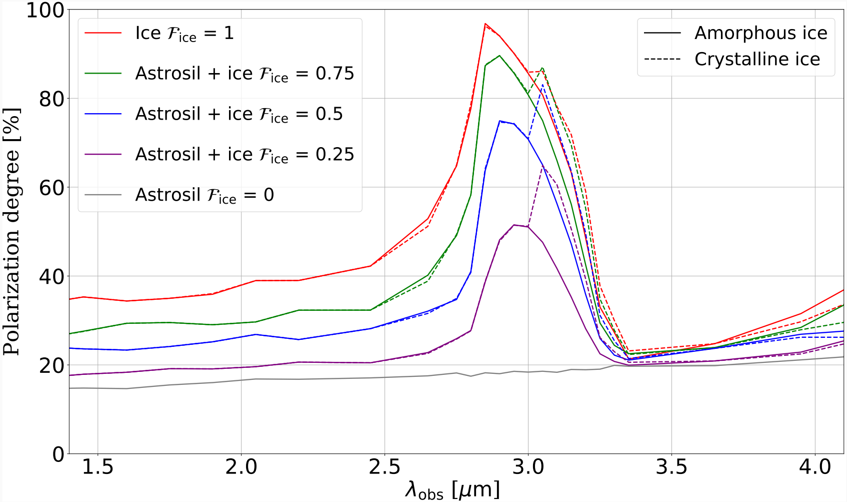

1-2. Polarization degree: Impact of $\mathcal{F}_{ice}$ in Astrosil + ice mixtures

Highly polarized radiation of 3 μm ice feature

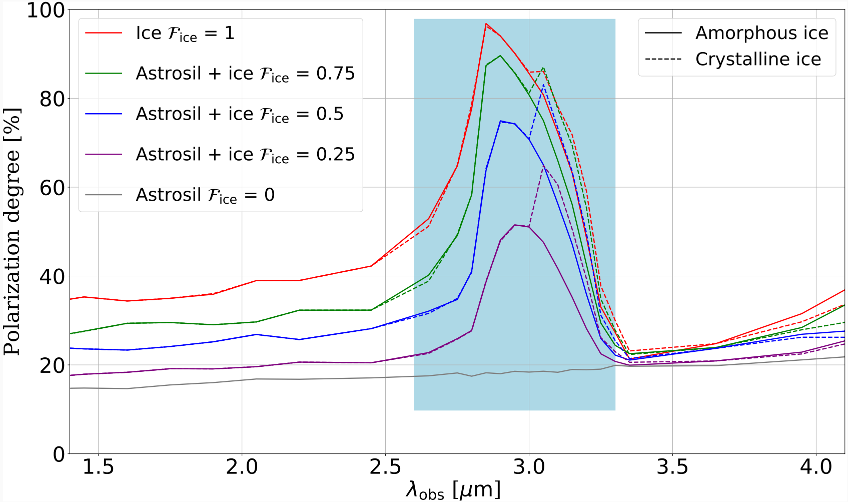

2-1. Spatially resolved images: Impact of ice destruction mechanism

Smaller difference with increasing observing wavelength.

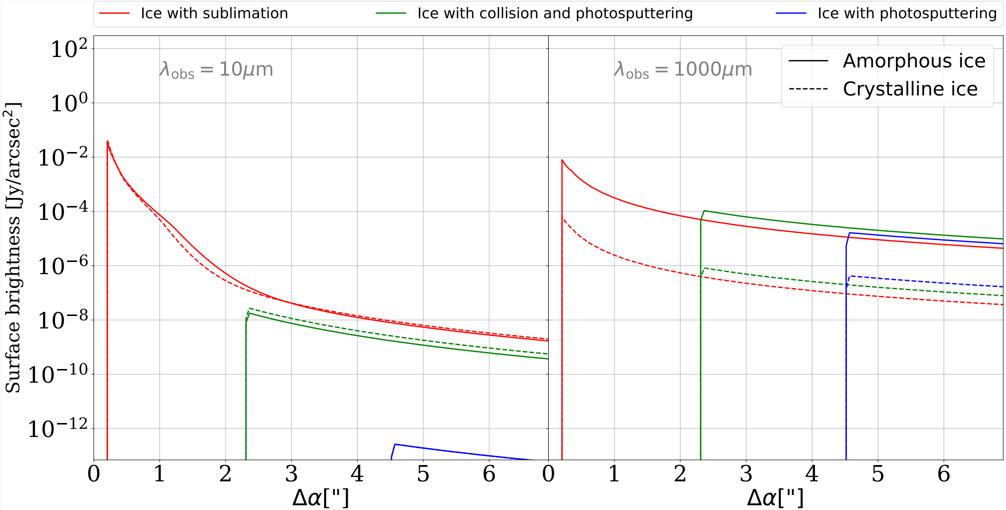

2-1. Spatially resolved images: Impact of $\mathcal{F}_{ice}$ in Astrosil + ice mixtures

The surface brightness transition at 10 μm due to the ice sublimation.

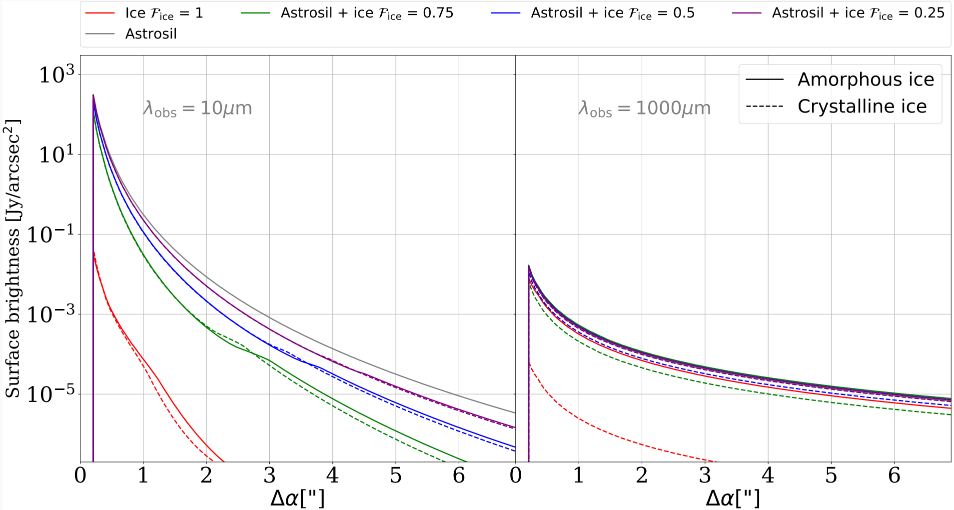

2-2. Tracing the ”ice survival line” of blowout grain size

The ice survival line $\propto$ chemical component, different shape of aggregates, and physical states (amorphousness vs crystallinity) of the icy-dust aggregates.

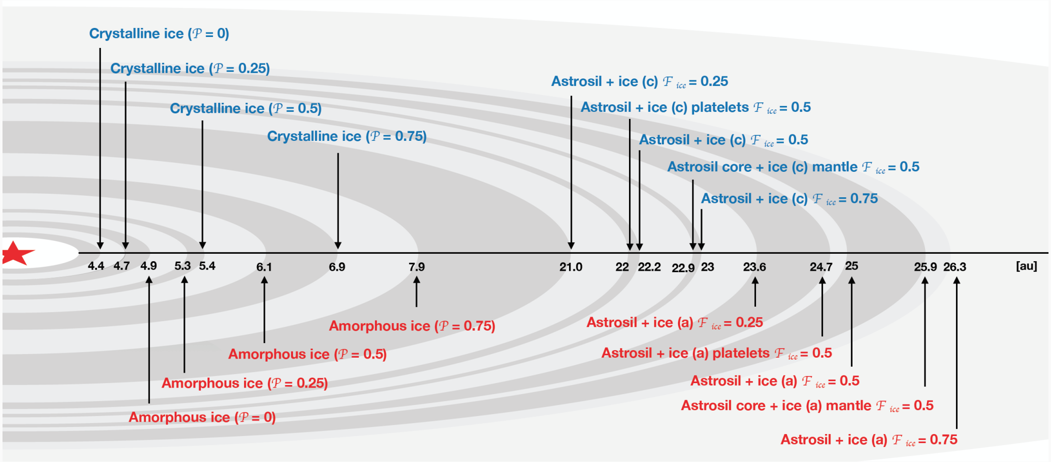

How do we constrain the detectability of water ice in debris disks?

Refractive indices (n & k) of water ice

Around 3 and 44 μm

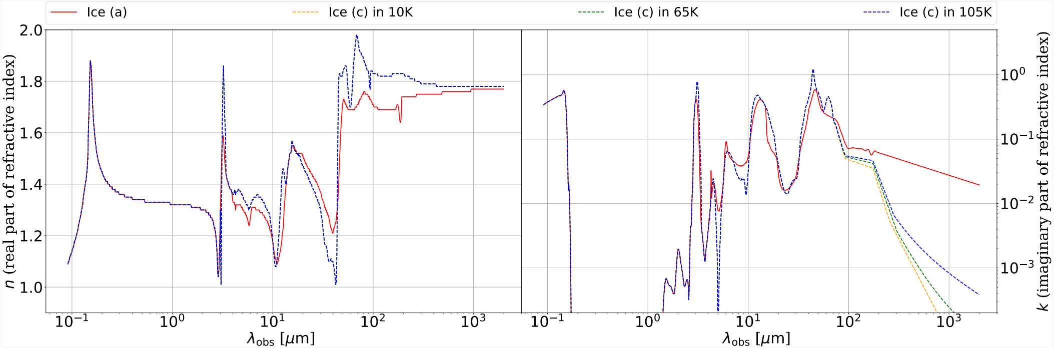

3-1. Evaluating the detectability of ice dust grains with JWST

Significantly increased ratio between surface brightness at 2.8 and 3.8 μm in the inner part of disks

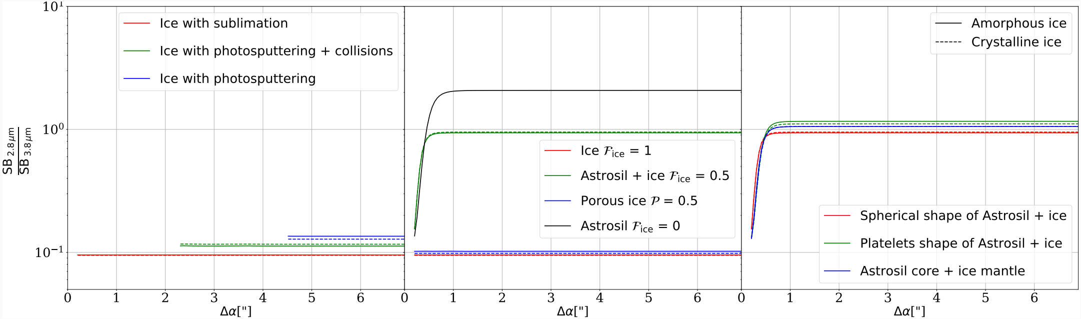

Nearly identical ratio between surface brightness at 35 μm and 44 μm for Astrosil-ice mixture

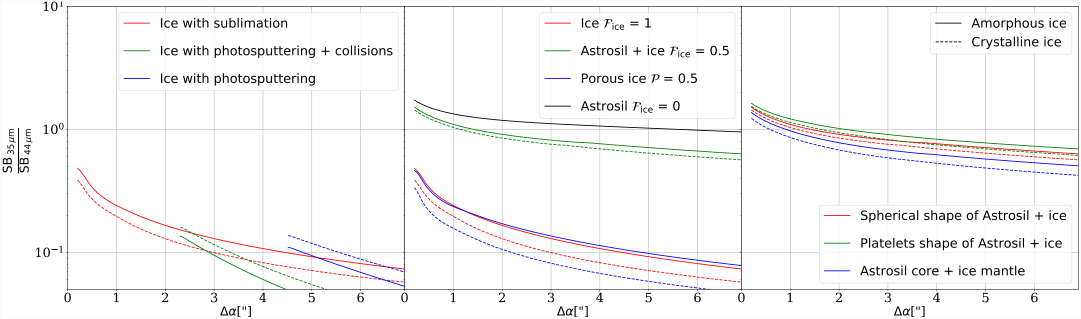

Take home messages: the feasibility to detect ice in debris disks

- Strong influence of the sublimation, collisions, and photosputtering on the observational appearance of debris disk systems
- Enhanced polarization levels in the 3 $\mu\mathrm{m}$ ice band for the ice-rich aggreagates
- The different ice survival line of debris disk system by the different physical states, a component of dust aggregates, and porosity
- Predictions on the feasibility to detect ice and spatially resolve characteristic structures with JWST and SPICA.

Take home messages: the feasibility to detect ice in debris disks

- Strong influence of the sublimation, collisions, and photosputtering on the observational appearance of debris disk systems
- Enhanced polarization levels in the 3 μm ice band for the ice-rich aggreagates
- The different ice survival line of debris disk system by the different physical states, a component of dust aggregates, and porosity
- Predictions on the feasibility to detect ice and spatially resolve characteristic structures with JWST and SPICA.

Thank you so much for your attention and happy holiday!

Extra pages

Introduction - Previous theories of icy-dust grains

- Surface density of solid matter increases beyond the snow line due to the increase of the icy dust mass, which enables to form a massive 10 earth-mass solid core of the gas giant (Hayashi et al. 1985).
- Icy planetesimals or comets bring the water to Earth (Morbidelli et al. 2000; Raymond et al. 2004) ?
- Water ice evaporation at the inner region of the disk brought the oxygen isotope anomaly seen in the meteorites (Yurimoto & Kuramoto 2004).

Introduction - Previous observations of icy-dust grains

- **Ice grain has been detected around protoplanetary disks!** 3 μm, 44 μm, and 62 μm water ice absorption & emission features. (Malfait et al. 1999; Molster et al. 2002; Terada et al. 2007; Terada & Tokunaga 2012; Aikawa et al. 2012).
- As for the debris disks, even the presence of ice grains is **not clearly established observationally**. A tentative detection of the 62 μm water ice emission feature is claimed (Chen et al. 2008). Some literatures concluded from comet studies that water-ice is not so abundant.

Method - *DMS* : Debris around Main-sequence Stars (Kim et al. 2018)

- Scattered light intensity and polarization maps:

$$W_\lambda^{\rm sca} = L_{\lambda,*} Q_\lambda^{\rm sca}(a) \frac{\pi a^2}{4\pi r^2} S_{11}(\theta) d\theta, \tag{1}$$

$$(W_\lambda^{\rm sca})_{\rm pol} = L_{\lambda,*} Q_\lambda^{\rm sca}(a) \frac{\pi a^2}{4\pi r^2} S_{12}(\theta) d\theta, \tag{2}$$

- Thermal re-emission maps:

$$W_\lambda^{\rm abs} = L_{\lambda,*} Q_\lambda^{\rm abs}(a) \frac{\pi a^2}{4\pi r^2}, \tag{3}$$

$$W_\lambda^{\rm re-emi} = 4\pi a^2 Q_\lambda^{\rm abs}(a) B_\lambda(T_{\rm g}), \tag{4}$$

- The distance from the star (the temperature of spherical dust grain):

$$r(T_{\rm g}) = \frac{R_*}{2} \sqrt{\frac{\int_0^\infty Q_\lambda^{\rm abs}(a) L_{\lambda,*} d\lambda}{\int_0^\infty Q_\lambda^{\rm abs}(a) B_\lambda(T_{\rm g})}}. \tag{5}$$

Method - *DMS*: Debris around Main-sequence Stars (Kim et al. 2018)

<table>
<tr><th>DMS code</th><th>Input</th><th>Output</th></tr>
<tr><td>With analytical disk models</td><td>- Stellar parameter : R_*, L_*, T_*
- Disk parameter : R_{in}, R_{out}, M_{total}
- Dust properties : species, ρ_{bulk}
- Geometry
- Density distribution
- Grain size distribution
- Observing wavelength
- #pixel, ΔT and #sub-volumes</td><td rowspan="2">- Images of thermal re-emission
- Images of scattering
- Images of polarized scattering

- Radial profile of images

- Spectral Energy distribution

- Temperature distribution</td></tr>
<tr><td>With particle distribution</td><td>- Stellar parameter : R_*, L_*, T_*
- Disk parameter : M_{total}
- Dust properties : species, ρ_{bulk}
- Geometry
- Observing wavelength</td></tr>
</table>

Method - complex refractive index (or optical constant) of a particle

- The complex permittivity $\varepsilon = m^2 = (n + ik)^2 = (n^2 - k^2) + i(2nk)$
  , where n is the real part of the refractive index (responsible for scattering), k is the imaginary part of the refractive index (responsible for absorption and emission).

- Both n and k depend on the wavelength and chemical composition. If k is equal to 0 at a given wavelength thus a particle does not absorb radiation at this wavelength.

Method - Effective medium theory (EMT)

- Effective medium approximations are descriptions of a medium (composite material) based on the properties and the relative fractions of its components and are derived from calculations.

- Maxwell Garnett approximation:

$$\left(\frac{\varepsilon_{\text{eff}} - \varepsilon_m}{\varepsilon_{\text{eff}} + 2\varepsilon_m}\right) = \delta_i \left(\frac{\varepsilon_i - \varepsilon_m}{\varepsilon_i + 2\varepsilon_m}\right) \tag{6}$$

, where ε_{eff} is the effective dielectric constant of the medium (i.e., the complex permittivity), ε_i is the one of the inclusions and ε_m is the one of the matrix; δ_i is the volume fraction of the inclusions.

- The **emc** code (Ossenkopf-Okada 1991) allows one to find the effective refractive index, e.g., the scattering and extinction behavior, for some rules of the effective medium approximations (e.g., Maxwell-Garnett rule used in this study), several kinds of inclusions of different shapes with different bulk materials.

2 ways of water ice destruction: Sublimation (Kobayashi et al. 2011)

- For the excesses are reproduced by a single temperature blackbody emission, the peak in the number of systems with a given T_{grain} occurs at 110 - 120K.
- Observed color change beyond 120 AU (Golimowski et al. 2006).
- Absence of warmer grains: as a result of sublimation of ice in the inner part of the disk?

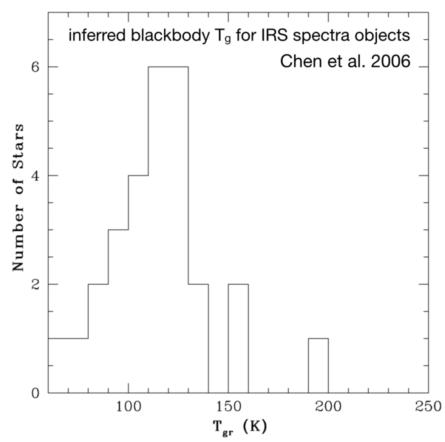

2 ways of water ice destruction: Sublimation (Kobayashi et al. 2011)

- For the excesses are reproduced by a single temperature blackbody emission, the peak in the number of systems with a given T_{grain} occurs at 110 - 120K.
- Observed color change beyond 120 AU (Golimowski et al. 2006).
- Absence of warmer grains: as a result of sublimation of ice in the inner part of the disk?

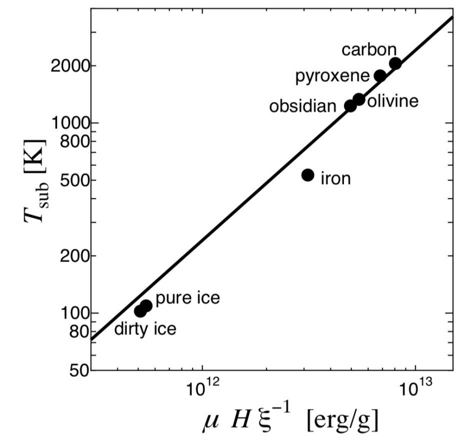

2 ways of water ice destruction: UV photosputtering (Grigorieva et al. 2007)

- **If the energetic photon is absorbed close to the surface, the molecules may escape.**
- Taking into account possible collisional activity slightly improves the situation.
- Herschel observation (Morales et al. 2016) shows the **larger minimum grains** ($f_{\mathrm{MB}} = a_{\mathrm{min}}/a_{\mathrm{BO}} \sim 5$).

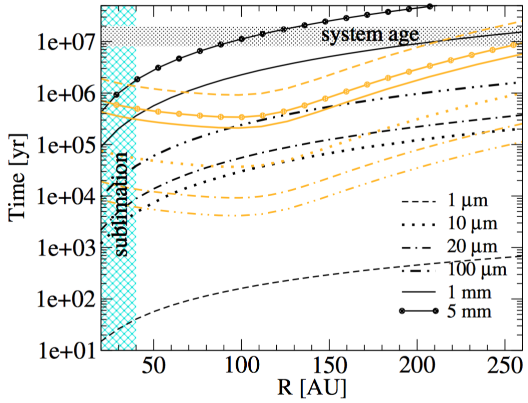

Chemical component (even vacumm) and physical states (amorphous vs crystallinity)

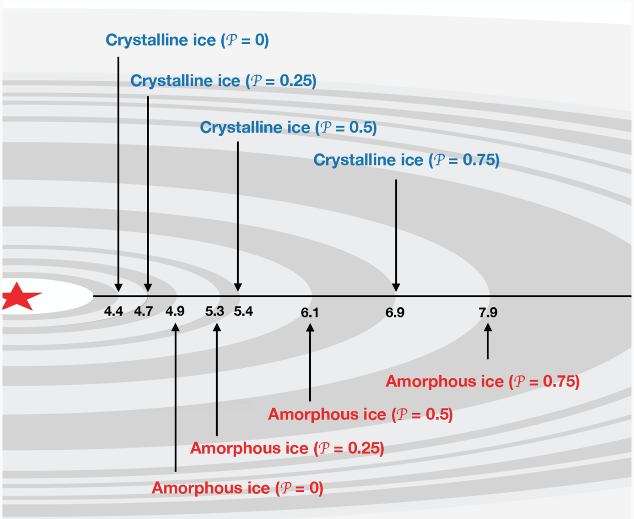

2-2. Tracing the ”ice survival line” of blowout grain size

Chemical component, different shape of aggregates, and physical states